Fabrication of Multiple Slanted Microstructures on Silica Glass by Laser-Induced Backside Wet Etching

Tadatake SATO[*1], Ryozo KUROSAKI[*1], Yoshizo KAWAGUCHI[*1], Aiko NARAZAKI[*1] and Hiroyuki NIINO[*1]

[*1] *Photonics Research Institute, National Institute of Advanced Industrial Science and Technology (AIST), Tsukuba Central 5, 1-1-1 Higashi, Tsukuba, Ibaraki 305-8565, Japan*
E-mail: sato-tadatake@aist.go.jp

Slanted microstructures were fabricated on silica glass by laser-induced backside wet etching (LIBWE) with gradual shift of the area irradiated by normal incidence. Slanted microtrenches with tilting angles up to about 30 degrees could be fabricated by lateral shift of the irradiated area with the speed of ~5.0 nm·pulse^{-1} under the conditions showing the vertical etching with rate of 7.0 - 11 nm·pulse^{-1}. Tilting angle could be controlled by the speed of lateral shift the irradiated area during the etching. Such structures were formed as a result of both lateral and vertical etching at the etch front. The trench structure fabricated by drastic shift of the irradiated area indicated that the etching of the sidewalls occurred at the area with height of around 400 nm.

DOI:10.2961/jlmn.2010.03.0014
Keywords: Laser-micromachining, LIBWE, deep trench with high aspect ratio, slanted structure

1. Introduction

Laser micromachining of transparent materials is widely studied as an important technique for fabricating micro electro-optical-mechanical system (MEOMS) components, microfluidic chips, and so on. The use of pulsed lasers are involved in several approaches, such as conventional UV laser ablation [1], vacuum UV laser processing [2,3], pulsed-laser generated X-ray [4], and femtosecond laser micromachining [1,5,6]. Apart from these direct processing methods, indirect processing methods have been proved to be effective means for precise and low-damage micromachining of hard and brittle transparent materials: in these methods, backside irradiation layout is generally employed. Laser light passing through the transparent materials to be etched is absorbed not by the materials but instead by a highly laser-absorbing media that covers the materials. We have developed laser-induced backside wet etching (LIBWE) as one of such indirect machining [7]. A highly concentrated organic dye solution such as acetone solution saturated with pyrene is employed as laser-absorbing media in this method. As far, microfabrications of various transparent materials with various laser-absorbing liquids have been reported from several research groups [8-25]. Schafeev and co-workers reported resemble approach using inorganic solution [26-28]; in this method, metal layer deposit by the laser irradiation contributes for the surface etching. Recently, similar approach was reported by Hong and co-workers [29]. Sugioka and co-workers developed the laser-induced plasma-assisted UV ablation (LIPPA) [30,31]. Laser induced backside dry etching (LIBDE) [32,33] and laser etching at surface adsorbed layer (LASEL) [34] are also studied. In these methods, thin metal layer and adsorbed layer from toluene vapor on glass are employed as laser-absorbing media, respectively.

Despite the intensive studies, the mechanism of LIBWE is still not fully understood. In initial stage of LIBWE, laser light passing through the glass is completely absorbed by the very thin liquid layer at the interface to form a transient photo-activated region. This region acts on the surface layer of the glass, resulting in etching as well as the generation of shockwaves and bubbles [12,22]. Meanwhile, the contribution of thin carbon layer generated by thermal degradation of heated solution to the etching process has been pointed out [11,14,15,20,22]. Moreover, the contribution of modified surface layer has been recently presented [17,18].

Fabrication of micro-devices often requires complex microstructures with high aspect ratios. Complex microstructures have been fabricated in glass materials by means of a two-step femtosecond laser-assisted etching process [35,36]. Although indirect machining is based on the phenomena at the interface between materials to be etched and laser-absorbing media, deep mirostructures can be fabricated in silica glass in only one step using LIBWE: deep trenches with an aspect ratio as high as 60 have been successfully fabricated [8]. Recently, we have succeeded to fabricate deep trenches with an aspect ratio over 100 [37].

Interestingly, inclined trenches have been fabricated by means of oblique incidence [38,39]. These results indicate that etch front in LIBWE proceeds in a direction parallel to the incidence of the laser beam. On the other hand, similar inclined trenches could be fabricated by gradually shifting the area irradiated by normal incidence during LIBWE [40]. Shafeev and coworkers reported the formation of inclined channels in a sapphire plate upon shifting the irradiated area, although the inclination was not controlled [26,27]. In this study, we investigated the fabrication of deep microtrenches including various inclined features by shifting the irradiated area. At the present method, the tilting angles of the inclined features can be controlled by stage motion. Therefore, multiple slanted microstructure can be fabricated.

2. Experimental

Microstructures were fabricated on synthetic silica glass plates (Tosoh SGM, ES grade, size: 2 × 2 cm, thickness: 2 or 0.5 mm) by the LIBWE employing acetone solution saturated with pyrene and a KrF excimer laser (Lambda Physik, Compex110, λ = 248 nm, FWHM ≈ 20 ns). Fluence and repetition rate were set to 1.0 J·cm^{-2}·pulse^{-1}, and 80 Hz, respectively. Microstructures were generated by using a mask projection system including beam homogenizer with nominal 1/8 demagnification (MicroLas, Vario-Las). By using photo-mask with a rectangular opening (80 × 8000 μm), a rectangular area at the liquid-solid interface with size of 10 × 1000 μm was irradiated for etching. The location of micromachining was controlled by a computer-controlled XYZ stage (Sigmatech Co., FS-1050), on which a sample composed of a glass plate and solution was mounted. The position of the sample was controlled with a resolution of ±0.2 μm. Shifting speed can be set with a resolution of 0.1 μm·s^{-1}. When etch depth becomes too large, the sample position must be shifted away from the projection lens to match the liquid-glass interface with image plane of the projection system [8]. Stage shifting conditions to optimize the imaging conditions were chosen as follows: initial irradiation was carried out for 5.0 s without shifting the stage, to compensate for the initial low etch rate, and then the stage was shifted away from the projection lens at a speed of 0.6 μm·s^{-1}. The shifting speed of the stage is smaller than the etch rate because patterned laser beam is imaged in focus at the glass-liquid interface through the silica glass with refractive index of n = 1.50841 at λ = 248 nm [41]. When the depth of trench becomes to be d, the position of the sample must be shifted by d/n to locate the etch front (bottom of the trench) at the position of image plane. For fabricating the inclined features, the sample position was gradually shifted in a direction perpendicular to the incidence of the laser beam as well.

To observe the cross-sectional images of the trenches, the glass plates on which trenches were fabricated were cut perpendicular to the long axis of the trenches. To cut at the center of trenches (1 mm length), guiding trenches (10 μm width and ca. 350 μm depth) were also prepared by the LIBWE. Cross-sectional images were obtained by a digital optical microscope (Keyence, VH-5500 with VHZ-100R) or a scanning electron microscope (SEM, Keyence, VK-7800).

3. Results and discussions

Microtrenches with 10 μm width and 1 mm length were fabricated by LIBWE employing a KrF excimer laser and saturated pyrene/acetone solution. Upon normal incidence without stage motion vertical deep trenches can be fabricated. Meanwhile, slanted structures are fabricated with shifting the irradiated area in a direction perpendicular to the laser incidence. The tilting angles of the slanted structures can be controlled by shifting speed of the irradiated area (v_{irr}) as followed.

3.1 Fabrication of slanted structures

A vertical trench with a depth of 21 μm was obtained by irradiation with 2400 pulses without shifting the stage (v_{irr} = 0 nm·pulse^{-1}), whereas inclined trenches were fabricated at 1.25 ≤ v_{irr} ≤ 3.75 nm·pulse^{-1} (Figs. 1(a), (b)). The tilting angles (θ) of the trenches fabricated with v_{irr} = 1.25, 2.50, and 3.75 nm·pulse^{-1} were estimated to be 9°, 18°, and 27°, respectively.

These θ values can be expressed by the ratio between the etch rate in the vertical (r_V) and lateral (r_L) directions (Fig. 2(a)), as shown in equation 1:

$$\tan\theta = \frac{r_L}{r_V} \qquad (1)$$

The initial r_V was estimated to be 7.0 nm·pulse^{-1} as described below. On the other hand, r_L should be equivalent to v_{irr}. From these values, θ values were calculated to be 10°, 20°, and 28°, respectively, and agreed fairly well with the experimental results. Slight deviation would be due to slight variation in r_V reflecting the difference of the conditions such as v_{irr}.

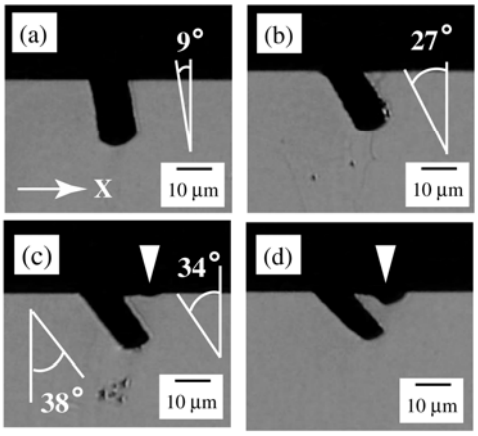

Fig. 1 Cross-sectional images of trenches prepared by irradiation with 2400 pulses. v_{irr} were (a) 1.25, (b) 3.75, (c) 5.00, and (d) 6.25 nm·pulse^{-1}. The white arrows indicate the direction of the shift of the irradiated area.

As shown in the figures, the bottoms of the trenches were not flat but round. Such round bottoms were also observed for the trenches without inclination (Figs 6(a)). The reasons of the formation of the round bottoms are not known yet. At the initial stage of etching, the etched surface was almost flat as reported by Zimmer et al.[42]. While the curvature of the bottom increases gradually with depth: the result indicates the difference in etch rates in center and near the sidewalls. This increase in curvature was observed at the trenches with depth up to about 15 μm. Above this depth, the curvature of the bottom stayed constant, indicating the same etch rate in center and near sidewalls. The depth where the change in curvature of the bottom surface observed corresponded to the depth where the change in etch rate was shown as described later. Given the relationship between etch rates shown in center and near sidewalls changing with depth, formation of round bottoms would be due to the difference in surrounding spatial conditions for the irradiated area. Moreover, formation of the

inclined features from the surface where the etched surface is almost flat indicates that the round bottom is not essential for the lateral etching.

The bottoms of the inclined features were not similar to those of vertical trenches. The bottoms have the shapes that would be formed by inclining the round bottom of vertical trenches. The inclinations of the bottoms seem to increase with θ although the precise inclination is difficult to evaluate because of their roundness.

When the inclined features were successfully fabricated, laser beam would irradiate only the bottom of the trenches, where the etching occurred, as illustrated in Fig. 2(a).

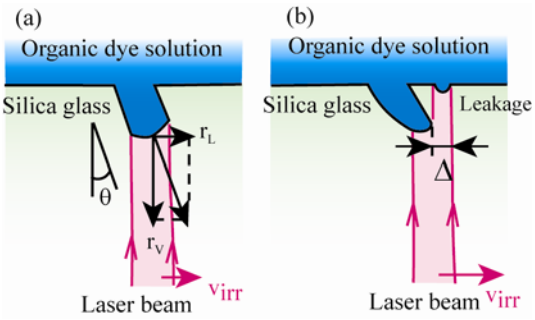

Fig. 2 Schematic illustration of (a) the fabrication of an inclined trench, and (b) the leakage of laser beam from the bottom of the trench under excess v_{irr}.

In contrast, when v_{irr} = 5.00 nm·pulse^{-1}, the surface of the glass was slightly etched as indicated by the white triangle in Fig. 1(c). Such surface etching was enhanced when v_{irr} was increased to 6.25 nm·pulse^{-1} (Fig. 1(d)). The surface etching was most likely done by laser reached to the surface, as illustrated in Fig. 2(b). The result indicates that there is an upper limit on r_L. When v_{irr} exceeds this upper limit ($r_{L,max}$), the distance between the right edge of the irradiated area and the right edge of the etched part, which is shown as Δ in Fig. 2(b), increases proportional to the irradiation time and the difference between v_{irr} and $r_{L,max}$. The laser with width of Δ was reached to the glass-liquid interface at the top surface. As shown in Fig. 3(b), the trenches with depth of around 140 μm could be fabricated without stage shift for optimizing the imaging conditions. In these trenches, the reduction of the width was observed in the region deeper than 80 μm. Therefore, the etching both at the surface and at the bottom of the trenches was done within the depth of focus (DOF) of the projection system in the present cases [43].

3.2 Estimation of vertical etch rate at various depth

In the present method, the θ values of the trenches here can be controlled by changing v_{irr}. The θ value is expressed by the ratio between r_V and r_L. Therefore, we investigated the rate r_V at various depths. Fig. 3(a) shows the etch depths of trenches fabricated with irradiation times of 160 to 2560 pulses. The rate r_V was constant for the trenches with depths up to 7 μm, but increased for those deeper than 10 μm. The initial r_V was estimated to be 7.0 nm·pulse^{-1} from the fitted line shown in Fig. 3(a).

The etch depths of trenches fabricated with irradiation times of 800 to 28000 pulses are shown as solid circles in Fig. 3(b). In this time region, r_V decreased gradually (solid circles), and then etching ceased completely at a trench depth of around 140 μm. These results indicate that the etch front exceeded the DOF of the projection system. As previously reported [8,39], when the etch depth becomes too large, the sample position must be shifted away from the projection lens so that the liquid-glass interface remains within DOF. By applying appropriate stage shifting conditions to optimize the imaging conditions, the etch depth increased linearly up to 28000 pulses as shown in Fig. 3(b) (open squares). For these trenches, r_V was estimated to be 11 nm·pulse^{-1}. This value is larger than the initial r_V. Increase in r_V is generally observed in deep trench fabrication by LIBWE [39]. As discussed above, the observed change in r_V shows correspondence to the change in the shape of bottoms of the trenches. Therefore, this change would be due to the difference in surrounding spatial conditions for the irradiated area as described earlier. This increase maybe due to existence of sidewalls around the photo-activated region, that is, the confinement of the photo-activated region inside the deep trenches caused an increase in r_V. At present, it was shown that this effect became remarkable in narrower trenches. Further studies are ongoing.

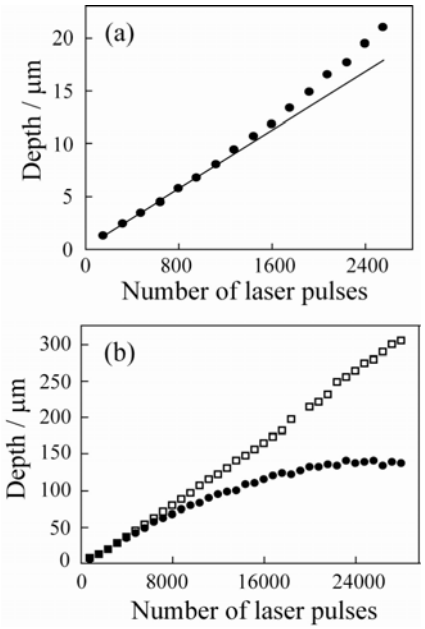

Fig. 3 Etch depth of 10-μm wide trenches fabricated with various irradiation times: (a) 160–2560 pulses, (b) 800–28000 pulses. Solid circles show the depths of trenches obtained without shifting the stage, whereas open squares shows the depths of trenches obtained with the stage shift to match the liquid-glass interface to the imaging plane.

3.3 Fabrication of multiple slanted structures

Using the conditions to maintain optimal imaging conditions, we examined the fabrication of the inclined sections in trenches deeper than 21 μm. First, a vertical trench with a depth of 21 μm was fabricated by irradiating with 2400 pulses. Then, to fabricate an inclined feature at the bottom of this trench, additional irradiation was applied while shifting the stage in both the X- and Y-directions. Fig. 4 shows cross-sectional images of trenches in which in-

clined features were fabricated by additional irradiation with 3120 pulses.

When v_{irr} was set to 5.00 nm·pulse^{-1}, an inclined feature was fabricated without reduction in this feature's width relative to the width of the original trench (Fig. 4(a)).

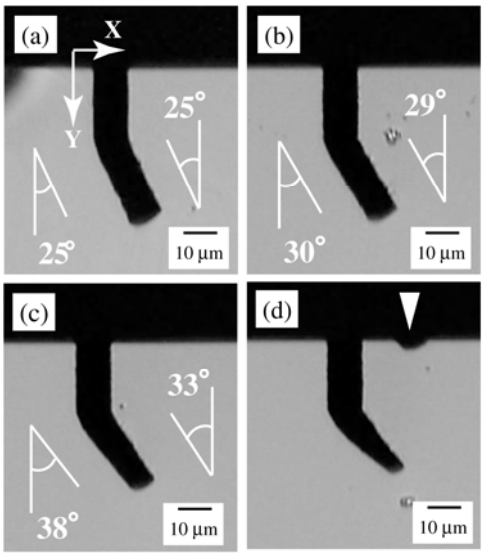

Fig. 4 Cross-sectional images of trenches with inclined features that were fabricated by additional irradiation with 3120 pulses. v_{irr} was set to (a) 5.00, (b) 6.25, (c) 7.50, and (d) 8.75 nm·pulse^{-1}. The white arrows indicate the direction of the shift of the irradiated area.

In contrast, a reduction in width was observed for an inclined section fabricated with v_{irr} = 7.50 nm·pulse^{-1} (Fig. 4(c)). However, surface etching caused by laser beam reached to the surface was not discernable, probably because the area irradiated by the laser reached to the surface was too small. The etch rate in LIBWE decreases with reducing in the irradiated area [15,25]. Size effect in fabrication of microtrenches is discussed later. Such surface etching was observed at $v_{irr} \geq$ 8.75 nm·pulse^{-1}, in addition to substantial width reduction relative to the original trench width (Fig. 4(d)). From these results, the tilting angle of 33° observed for the right sidewall in Fig. 4(c) would be close to $r_{L,max}$ under the present conditions. This tilting angle means $r_{L,max}$ is about 65% of r_V = 11, or 7.0 nm·pulse^{-1}. Therefore, slanted structures with tilting angles of up to ca. 30° can be fabricated at the present conditions.

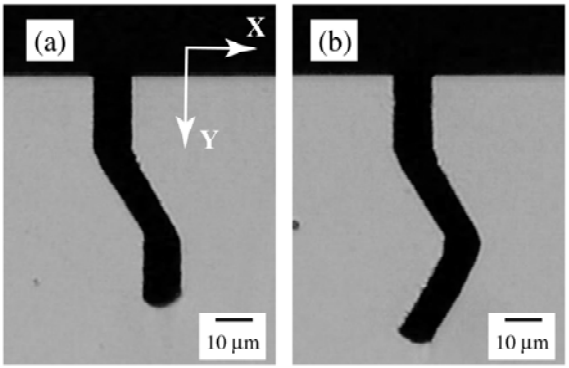

Fig. 5 Cross-sectional images of multiple slanted trenches fabricated by stage motions.

As described previously, θ could be changed within a single deep trench by shifting the stage and thus shifting the irradiated area. By changing the shifting speed v_{irr}, the θ values of the inclined features were flexibly controlled. Fig. 5 shows cross-sectional images of multiple slanted deep trenches. As shown in the figure, the various inclined parts were freely connected. Thus, flexible structure formation deep beneath the surface of the silica glass can be achieved with the LIBWE method.

3.4 Trenches fabricated by large shift of the irradiated area

As discussed above, slanted structures are fabricated as a result of both lateral and vertical etching at the etch front. To observe this lateral etching for the sidewall definitely, drastic shift of the irradiated area was examined. Fig. 6(b) shows the cross-sectional image of the trench fabricated by two steps: (1) vertical trench was fabricated by irradiation with 2400 pulses, trench shown in Fig. 6(a) was obtained, (2) additional irradiation with 3200 pulses was applied after shifting of the irradiated area to the right by 5 μm.

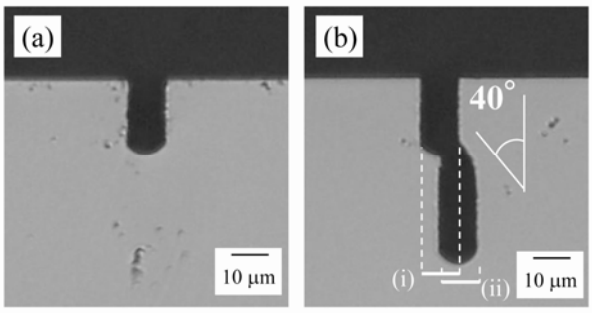

Fig. 6 Cross-sectional image of the trench with 10 μm (a) fabricated by only (i) initial irradiation and (b) that fabricated with (ii) successive irradiation after shifting irradiation area by 5 μm.

The formation of this structure can be explained on the basis of the lateral etching and the size effect in LIBWE. As reported from the several group [15,25], there is a size effect in LIBWE, that is, the etch rate decreases with decreasing the size of the etching. Surface etch rate for the trenches with 5 μm width were estimated to be 4.0 nm·pulse^{-1}. This rate is smaller than that for trenches with 10 μm width (7.0 nm·pulse^{-1}).

Just after the shift of the irradiated area, the half of laser light (5 μm width) irradiates the bottom of the trench, and remaining half reaches to the surface. At the bottom of the trench, the etching occurs to both the vertical and lateral directions to form inclined sidewall (Fig. 7). The initial tilting angle of the inclined sidewall was estimated to be ca. 40°. This angle is close to the observed maximum tilting angle in fabrication of multiple slanted trenches. This result suggests that this inclined sidewall is formed by the similar mechanism with the fabrication of the multiple slanted structures.

As a result of the lateral etching, the width of the trench increased continuously at the bottom and then finally recovered to the original width. By increasing the width, the

etch rate increased as well. Whereas, this increase of width at the bottom resulted in the decrease in the width of the light reaching to the surface, which resulted in decrease of etch rate. Therefore, the etching at the surface remains negligibly small. Depth of the etched part on the surface was measured to be a few μm.

As discussed above, the structure shown in Fig. 6(b) would be formed as a result of the lateral etching. If the lateral etching was done as the etching of perpendicular sidewalls by photo-activated region generated in the solution as shown in Fig. 7, the location of the bending point of sidewall ((ii) in Fig. 7) and the location of the bottom edge of the original vertical trench ((iii) in Fig. 7) should be different. And this difference indicates the effective area ((v) in Fig. 7) where etching of the perpendicular sidewall occurs.

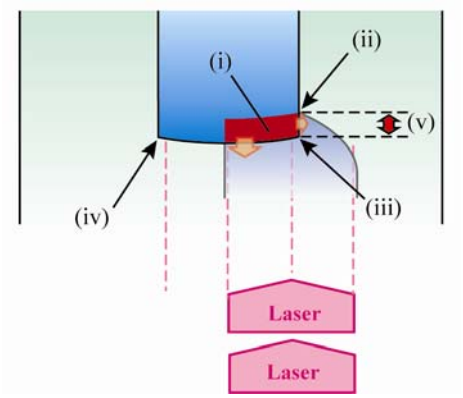

Fig. 7 Schematic drawing the photo-activated region generated at the bottom of trench just after the shift of the irradiated area. (i) photo-activated region, (ii) bending point of sidewall, (iii) bottom edge of the original vertical trench, (iv) untouched bottom edge, (v) height for the area where the effective sidewall etching occurs.

Therefore, the location of the positions of bending point of the sidewalls and the positions of the bottom edge of original vertical trenches were carefully examined, since relatively large experimental error cannot be avoided in case of fabrication of deep trenches that were fabricated by thousands of laser pulses. To overcome the problem of reproducibility, 54 original vertical trenches and 46 trenches with shifted irradiation were prepared and examined. The half of the 46 trenches were fabricated with shifted the irradiated area to the right, while the other trenches were fabricated with shifted to the left. Depths of the bending point or that of bottom edge were measured as shown in Fig. 8. The results are summarized in Table 1.

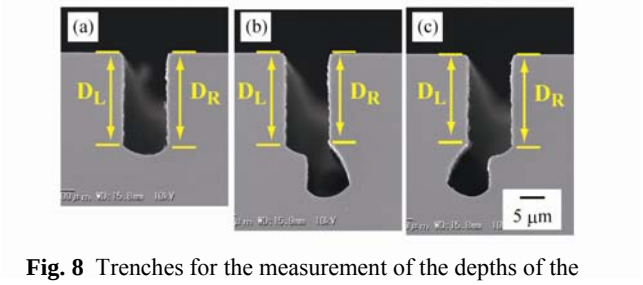

Fig. 8 Trenches for the measurement of the depths of the bending point / bottom edge of the trenches. (a) original vertical trench, and trenches with additional shifted irradiation (b) to the right and (c) to the left.

Table 1 Depths of the bending point / bottom edge of the trenches

	Original vertical trench	Trenches with shifted irradiated area	
		to the right	to the left
D_L /μm	18.53 ±0.25	18.51 ±0.28 (-0.02)	18.20 ±0.30* (-0.33)
D_R /μm	18.55 ±0.25	18.13 ±0.27* (-0.42)	18.57 ±0.28 (+0.02)

* Depths of the bending point

The depths of the untouched bottom edge ((iv) in Fig. 7) are almost similar to those of the corresponding edges of the original vertical trenches (-0.02 and +0.02 μm with experimental variance of ±0.28 μm), while the depths of bending point are smaller than that of bottom edge of the original vertical trenches by 0.33 and 0.42 μm, with experimental variance of ±0.30 and ±0.27μm, respectively. Almost similar size of experimental variance was observed for all cases, while bending points selectively shows position difference of 0.33 and 0.42 μm. Therefore, these values correspond to the height of the area where etching of the perpendicular sidewall occurs. This limited size of the area might be an origin of the upper limit in r_L.

Perpendicular sidewalls would be difficult to be etched by laser beam proceeding parallel to them. Moreover, the observed sizes of 0.33 and 0.42 μm are larger than the thermal diffusion length of the silica glass (56.6 nm [40]) . Therefore, the etching of perpendicular sidewalls is possibly induced by the action of photo-activated region generated in the solution contacting with glass surface. Details of action can be speculated as followed: the initial heating of the material to be etched is induced by absorption of laser energy by laser-absorbing media: not only the dye solution but adsorbed carbon layer or the surface modified layer [17] can act as the laser absorbing media. This heating forms molten surface layer at the irradiated area as well as transient super-heated liquid at the liquid-glass interface; the photo-activated region. The first action of this region would be heat exchange with surface. If the glass surface is more heated by the surface layers, it would heat up the solution. Since the activated region should have finite thickness, in this stage, its action affect not only on the irradiated surface but also on the sidewalls contacting to the region. This would form molten layer on the sidewalls. As a successive action of the region, it formed high-pressure vapor acting to the molten surface to remove it as proposed by Hopp et al. [44]. This action would affect on the molten part on the sidewalls as well. As a result, the etching occurs at the perpendicular sidewalls as well as irradiated surface. When the irradiated area is not shifted in the lateral direction, the action of activated region to the sidewalls would stay constant. As a result, vertical trenches can be fabricated. The existence of this action can be seen as slight variance in widths of trenches as reported previously [40].

While, it can be clearly seen as inclined structure formation when the irradiated area is shifted.

4. Conclusions

Slanted structures were successively fabricated from the surface of glass or from the bottoms of vertical microtrenches by gradual shift of the irradiated area in a direction perpendicular to the incidence of the laser beam. Tilting angles of the inclined features could be flexibly controlled by the shifting speed of the irradiated area: slanted structures with tilting angles of up to ca. 30° can be fabricated at the present conditions. Since the tilting angle can be changed in fabrication of one deep trench, multiple slanted structures can be fabricated by this method.

The trench structure fabricated by drastic shift of the irradiated area indicated that the etching of the perpendicular sidewalls occurred at the area with height of around 400 nm. This result indicates that the etching of perpendicular sidewalls would be due to the action of photo-activated region generated in the solution.

References

[1] J. Ihlemann, B. Wolff, P. Simon: Appl. Phys. A, 54, (1992) 363.

[2] P. R. Herman, R. S. Marjoribanks, A. Oettl, K. Chen, I. Konovalov, S. Ness: Appl. Surf. Sci., 154-155, (2000) 577.

[3] K. Sugioka, S. Wada, H. Tashiro, K. Toyoda, A. Nakamura: Appl. Phys. Lett., 65, (1994) 1510.

[4] T. Makimura, S. Uchida, K. Murakami, H. Niino: Appl. Phys. Lett., 89, (2006) 101118.

[5] F. He, Y. Cheng, L. Qiao, C. Wang, Z. Xu, K. Sugioka, K. Midorikawa, J. Wu: Appl. Phys. Lett., 96, (2010) 041108.

[6] H. Varel, D. Ashkenasi, A. Rosenfeld, M. Wähmer, E. E. B. Campbell, Appl. Phys. A, 65, (1997) 367.

[7] J. Wang, H. Niino, and A. Yabe: Appl. Phys. A 68 (1999) 111.

[8] Y. Kawaguchi, T. Sato, A. Narazaki, R. Kurosaki, H. Niino: Jpn. J. Appl. Phys., 44, (2005) L176.

[9] H. Niino, Y. Yasui, X. Ding, A. Narazaki, T. Sato, Y. Kawaguchi, A. Yabe: J. Photochem. Photobiol. A: Chem., 158, (2003) 179.

[10] X. Ding, Y. Yasui, Y. Kawaguchi, H. Niino, A. Yabe: Appl. Phys. A, 75, (2002) 437.

[11] X. Ding, T. Sato, Y. Kawaguchi, H. Niino: Jpn. J. Appl. Phys., 42, (2003) L176.

[12] H. Niino, Y. Kawaguchi, T. Sato, A. Narazaki, T. Gumpenberger, R. Kurosaki: Appl. Surf. Sci., 252, (2006) 4387.

[13] R. Böhme, A. Braun, K. Zimmer: Appl. Surf. Sci., 196, (2002) 276.

[14] R. Böhme, A. Braun, K. Zimmer: Appl. Surf. Sci., 208-209, (2003) 199.

[15] R. Böhme, K. Zimmer: Appl. Surf. Sci., 247, (2005) 256.

[16] K. Zimmer, R. Böhme, D. Ruthe, B. Raushenbach: Appl. Surf. Sci., 84, (2006) 455.

[17] K. Zimmer, R. Böhme, D. Ruthe, B. Raushenbach: Appl. Phys. A, 253, (2007) 6588.

[18] K. Zimmer, M. Ehrhardt, R. Böhme: J. Appl. Phys., 107, (2010) 034908.

[19] G. Kopitkovas, T. Lippert, C. David, S. Canulescu, A. Wokaun, J. Gobrecht: Micloelectron., 67-68, (2003) 438.

[20] G. Kopitkovas, V. Deckert, T. Lippert, F. Raimondi, C. W. Schneider, A. Wokaun: Phys. Chem. Chem. Phys., 10, (2008) 3195.

[21] C. Vass, K. Osvay, T. Veso, B. Hopp, Z. Bor: Appl. Phys. A 93, (2008) 69.

[22] C. Vass, T. Smausz, B. Hopp: J. Phys. D: Appl. Phys., 37, (2004) 2449.

[23] J. Chen, M. Yen, W. Hsu, J. Jhang, T. Yang: J. Micromech. Microeng. 16, (2006) 2420.

[24] K. Fujita, T. Hashimoto, K. Samonji, J. S. Speck, S. Nakamura: J. Cryst. Growth, 272, (2004) 370.

[25] T. Lee, D. Jang, D. Ahn, D. Kim: J. Appl. Phys., 107, (2010) 033112.

[26] S. I. Dolgaev, A. A. Lyalin, A. V. Simakin, G. A. Shafeev: Quantum Electron., 26, (1996) 65.

[27] S. I. Dolgaev, A. A. Lyalin, A. V. Simakin, G. A. Shafeev: Appl. Surf. Sci., 96-98, (1996) 491.

[28] A. V. Simakin, E. N. Lonbin, G. A. Shafeev, Quantum Electron. 30, (2000), 263.

[29] Z. Q. Huang, M. H. Hong, T. B. M. Do, Q. Y. Lin: Appl. Phys. A: 93, (2008) 159.

[30] J. Zhang, K. Sugioka, K. Midorikawa: Appl. Phys. A, 67, (1998) 545.

[31] Y. Hanada, K. Sugioka, I. Miyamoto, K. Midorikawa: Appl. Surf. Sci., 248, (2005) 276.

[32] B. Hopp, Cs Vass, T. Smarsz: Appl. Surf. Sci., 253, (2007) 7922.

[33] R. Böhme, K. Zimmer, B. Rauschenbach: Appl. Phys. A, 82, (2006) 325.

[34] R. Böhme, K. Zimmer: Appl. Surf. Sci., 239, (2004) 109.

[35] S. Matsuo, S. Kiyama, Y. Shichijo, T. Tomita, S. Hashimoto, Y. Hosokawa, and H. Masuhara: Appl. Phys. Lett., 93, (2008) 051107.

[36] Z. Wang, K. Sugioka, and K. Midorikawa: Appl. Phys. A, 93, (2008) 225.

[37] T. Sato, R. Kurosaki, A. Narazaki, Y. Kawaguchi, H. Niino: Proc. SPIE, 7584 (2010) 758408.

[38] H. Niino, Y. Kawaguchi, T. Sato, A. Narazaki, and R. Kurosaki: Appl. Surf. Sci. 253 (2007) 8287.

[39] Y. Kawaguchi, T. Sato, A. Narazaki, R. Kurosaki, and H. Niino: J. Photochem. Photobiol. A: Chem. 182 (2006) 319.

[40] T. Sato, R. Kurosaki, A. Narazaki, Y. Kawaguchi, H. Niino: Appl. Phys. A, 101 (2010) 319.

[41] E. D. Palik, Ed., "Handbook of Optical Constants of Solid," Academic Press, London, 1985.

[42] K. Zimmer, R. Böhme: Appl. Surf. Sci., 243, (2005) 415.

[43] For the imaging system, the size of DOF is not formulated as for the Gaussian beam. It depends on the tolerance of the size and shape variance; the larger pattern has apparently the longer DOF. For fabrication of 10-μm wide trench, almost homogeneous etch rate is shown in the range of □.□̃μm. Beyond this range, etch rate decreased drastically. Therefore, this range can be considered as DOF.

[44]B. Hopp, T. Smausz, T. Csizmadia, Cs. Vass, T. Csákó, G. Szabóo J. Laser Micro/Nanoeng., 5, (2010) 80.

(Received: June 7 , 2010, Accepted: November 18, 2010)